

A DEDICATED THz BEAMLINE AT DELTA*

M. Höner, P. Ungelenk[†],

M. Bakr, H. Huck, S. Khan, R. Molo, A. Nowaczyk, A. Schick, M. Zeinalzadeh,

Center for Synchrotron Radiation (DELTA), TU Dortmund University, 44221 Dortmund, Germany

Abstract

As a consequence of the new radiation source for ultrashort VUV pulses at DELTA, which is based on the interaction of electrons with fs laser pulses, coherent THz radiation is emitted. Simulations of the laser-electron interaction, particle dynamics and radiation spectrum, as well as the optical and mechanical design of a dedicated THz beamline are presented. First experimental results including laser-electron overlap diagnostics and characterization of the THz radiation are discussed.

INTRODUCTION

DELTA is a synchrotron light source with a beam energy of 1.5 GeV, a beam current up to 130 mA in multi-bunch mode, and a revolution frequency of 2.6 MHz. A sketch of its layout is shown in Fig. 1.

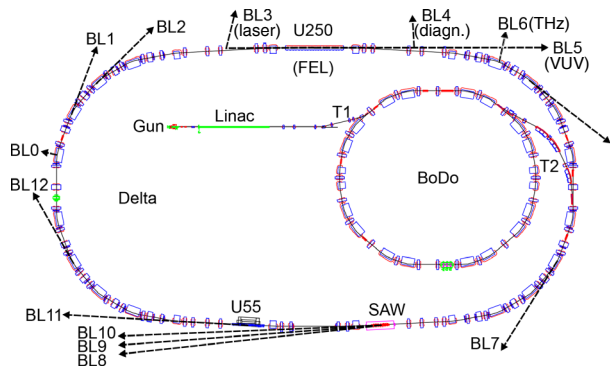


Figure 1: Sketch of the DELTA facility.

A new radiation source for ultrashort VUV pulses based on the Coherent Harmonic Generation (CHG) scheme is currently being commissioned [1, 2]. Caused by the interaction with a co-propagating laser pulse in the existing undulator U250, an energy modulation is imprinted onto a small section of the electron bunch, which is then converted into a micro-bunched electron distribution by a dispersive chicane at the center of the U250. These microbunches emit coherent radiation at harmonics of the original laser wavelength within the second half of the U250. The off-energy electrons then travel on dispersive orbits through the subsequent magnet lattice, causing the formation of a sub-picosecond dip in the longitudinal electron density. This gives rise to the emission of coherent THz pulses [3] into a new dedicated beamline (BL6).

* Work supported by DFG, BMBF, and by the Federal State NRW
[†] markus.hoener@tu-dortmund.de, peter.ungelenk@tu-dortmund.de

SIMULATIONS

Laser-Electron Interaction

In order to extract coherent THz radiation downstream of the U250, a new beamline had to be constructed. Its optimum position was determined by simulations. The interaction of the laser pulse and the electrons is simulated by numerically integrating the electrons' energy change due to a Gaussian laser pulse. Figure 2 shows a part of the longitudinal phase space of the electron bunch after the energy modulation. Using a laser pulse energy of 1.5 mJ as an example, the amplitude of the modulation amounts to 0.9% of the beam energy of 1.5 GeV.

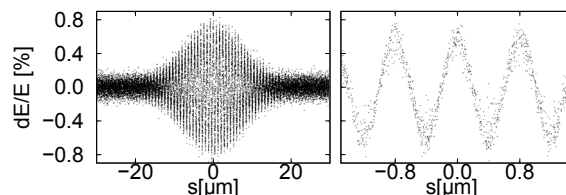


Figure 2: Part of the longitudinal phase space after the interaction of electrons with a fs laser pulse (a). The detailed view (b) shows the periodicity of the modulation corresponding to the laser wavelength.

Particle Tracking

Tracking simulations confirm the development of a dip in the longitudinal electron density. An optimum shape (most narrow and deep) is reached inside the third dipole after the U250. It can be described by the sum of two zero-centered Gaussian distributions (Fig. 3) with widths of 0.10 mm and 0.05 mm (FWHM), respectively, corresponding to roughly 1/1000 of the duration of the whole bunch (85 ps).

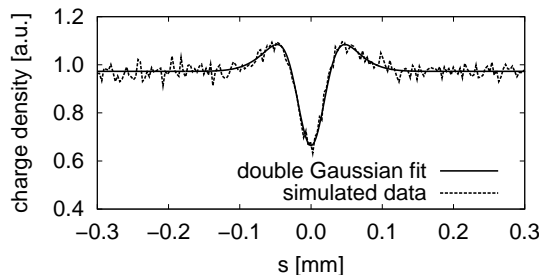


Figure 3: Part of the longitudinal charge density inside the third dipole following the U250 undulator.

Spectral and Angular Distribution

The total synchrotron radiation power of an electron bunch $P(\nu)$ can be described by

$$P(\nu) = P_e(\nu)N_e [1 + (N_e - 1)g^2(\nu)], \quad (1)$$

where $P_e(\nu)$ is the spectral power distribution of a single electron, N_e is the number of electrons inside the bunch, and $g(\nu)$ is the normalized Fourier transform of the longitudinal electron density [4]. The sub-picosecond dip predicted by the tracking simulations gives rise to coherent radiation in the range of 200 GHz to 8 THz (Fig. 4). The coherent amplification below 10 GHz, given by the bunch length, and the incoherent x-ray radiation will be suppressed by the vacuum chamber cutoff or absorbed by a water cooled copper mirror. The dipole fan provides an even distribution in the horizontal plane, whereas the vertical angular distribution of the THz radiation is given by the inset in Fig. 4.

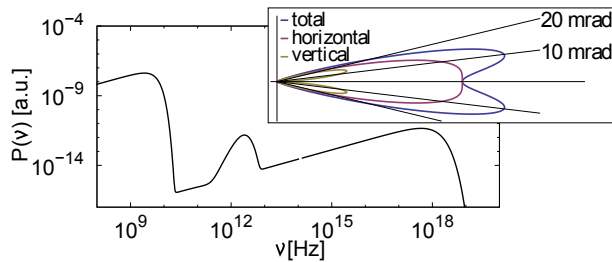


Figure 4: Total estimated spectrum at the THz beamline. The inset shows the vertical angular distribution divided into horizontal and vertical polarization directions.

Beamline Optics

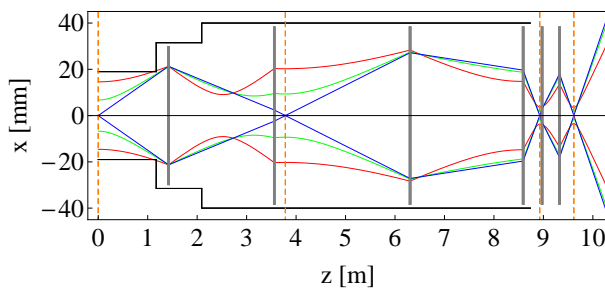


Figure 5: Transverse beam size x along the longitudinal coordinate z inside the THz beamline, shown for three wavelengths and initial beam waist sizes.

Six aluminium mirrors are used to transfer the THz radiation to the experimental station. Because of its long wavelength compared to x-rays or even visible light, diffraction effects have to be taken into account. The wavelength dependence of the waist positions is avoided (orange dashed lines in Fig. 5) by the use of three Gaussian telescopes [5]. Each of the mirrors has a toroidal surface to compensate spherical astigmatism due to the 90-degree deflections.

DESIGN AND ASSEMBLY

The specific design of the beamline and the positioning of the mirrors is displayed in Fig. 6. The construction was done during March 2011. The first laser-induced THz signal was detected at the end of June 2011.

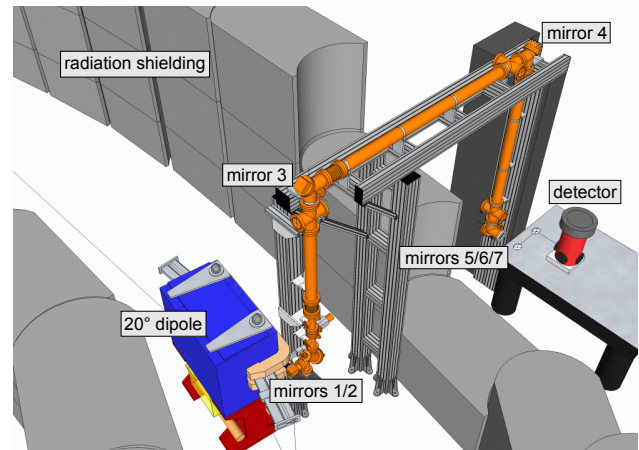


Figure 6: Overview of the THz beamline, comprising an evacuated beampipe (orange) and a support structure.

FIRST EXPERIMENTAL RESULTS

Multi-Turn Signal Shape

Figure 7 shows the THz signal shape from one laser shot acquired with an oscilloscope of 1 GHz bandwidth. Although the bolometer (bandwidth 1 MHz) cannot resolve single turns in DELTA (revolution frequency 2.6 MHz), the asymmetry of the pulse suggests an influence from subsequent turns. This is confirmed by a Gaussian fit for exponentially decaying signals from three successive revolutions at 0 ns, 384 ns, and 768 ns.

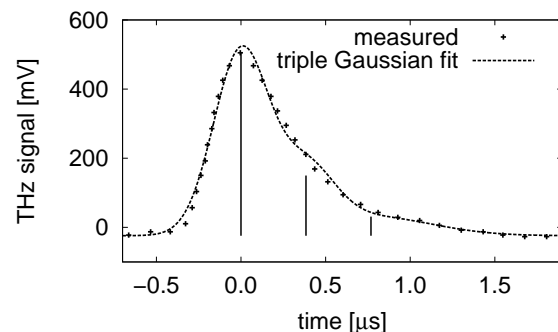


Figure 7: Time domain THz signal fitted by three Gaussians with their centers and amplitudes indicated by the vertical lines.

Longitudinal Overlap

Figure 8 shows the THz signal versus different delays between the electron bunch and the laser pulse. The width

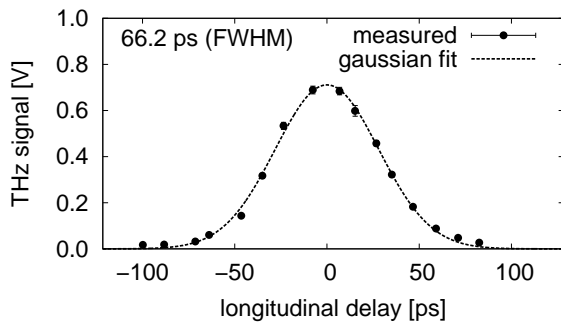


Figure 8: THz signal vs. longitudinal delay between the laser pulse and the center of the electron bunch.

of 66 ps (FWHM) is close to the square root of the natural bunch length of 85 ps [6].

Modulator Strength

The interaction of the laser with the electrons depends on the modulator’s resonance wavelength given by

$$\lambda_{\text{mod}} = \frac{\lambda_U}{2\gamma^2} \left(1 + \frac{K^2}{2} \right), \quad (2)$$

where γ is the Lorentz factor, λ_U is the period length of the modulator and K is the undulator parameter. Figure 9 shows the THz signal for three different scans of the modulator wavelength λ_U . As expected, the maximum THz signal is gained, if the undulator is tuned to the laser wavelength $\lambda_L = 795$ nm.

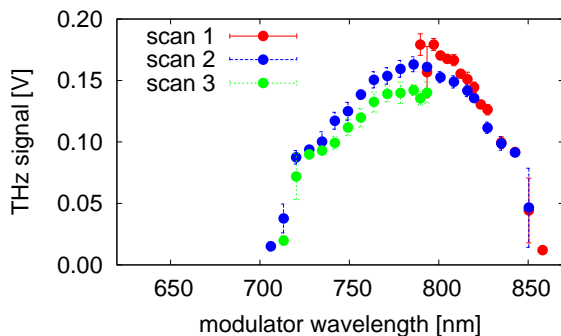


Figure 9: Dependence of the THz signal on the strength of the first part of the U250 undulator (modulator), here expressed by its fundamental wavelength.

Dependence on the Beam Current

The beam-current dependence (Fig. 10) is measured (a) in standard multi-bunch mode without and (b) in single-bunch mode with laser-induced energy modulation. In compliance with Eq. 1, the incoherent THz radiation is proportional to the beam current, whereas the coherent signal is proportional to the square of the bunch current.

02 Synchrotron Light Sources and FELs

A05 Synchrotron Radiation Facilities

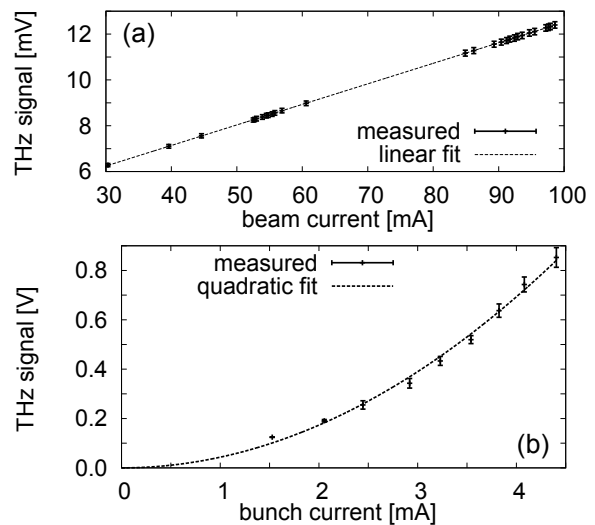


Figure 10: Incoherent THz signal vs. beam current (a) and laser-induced THz signal vs. bunch current (b).

OUTLOOK

Whereas the first experimental results were obtained within special machine shifts, CHG signals and laser-induced THz signals have been produced in standard user operation by now. In the near future, an upgrade including further automation and a THz spectrometer will take place. The goal is a user facility with high availability for ultrashort laser, VUV and THz pulses.

Possible applications of the THz beamline in the field of accelerator physics include laser-electron overlap diagnostics, bunch profile measurements and investigation of microbunching instabilities. Condensed matter physics profits from synchronized laser, VUV and THz pulses, allowing spectroscopy of weak bonds in semiconductors, superconductors and biomolecules as well as pump-probe studies of fast transition processes in the picosecond regime.

ACKNOWLEDGMENTS

It is a pleasure to thank our colleagues at DELTA and the Faculty of Physics for their continuous support. The project has profited from the expertise of our colleagues at HZB, MLS, DESY, KIT, and SLS.

REFERENCES

- [1] A. Schick et al., this conference.
- [2] S. Khan, Proc. PAC’09, Vancouver (2009), 1144.
- [3] K. Holldack, Proc. EPAC’04, Lucerne (2004), 2284.
- [4] H. Wiedemann, “Particle Accelerator Physics”, Springer, 3rd ed., 2007, p. 781.
- [5] N. Kaempfer, “THz-Optik”, University of Bern, 2006, http://www.iapmw.unibe.ch/teaching/vorlesungen/submm_optik/.
- [6] D. Schirmer, DELTA Int. Rep. 001-05, University of Dortmund, 2009.